ANTHROPOLOGY

The second century CE Roman watermills of Barbegal: Unraveling the enigma of one of the oldest industrial complexes

Gül Sürmelihindi[1], Philippe Leveau[2], Christoph Spötl[3], Vincent Bernard[4], Cees W. Passchier[1]*

The second century CE Roman watermill complex of Barbegal, France, is regarded as one of the first industrial complexes in human history. The 16 water wheels are no longer extant as all woodwork has decayed. However, carbonate deposits precipitated from water during operation of the mills forming casts on the woodwork. These casts are preserved in fragments and provide unique insights into the frequency of use and maintenance of the mills, and even into the structure of the water wheel chambers. Stable isotope time series of carbonate deposits reveal that the mill activity was regularly interrupted for several months. This strongly suggests that the mill complex was not used for a steady supply of flour to a major population center, as previously thought, but likely served to produce nonperishable hardtack for the nearby harbors.

INTRODUCTION

The Greco-Roman world has been presented by many scholars as an example of a society that was stagnant in terms of technological innovation and development, accrediting the idea that, although an ancient invention, watermills were first used on an industrial scale in medieval times (*1*–*4*). The scarcity of written sources on this subject in antiquity, for example, by Strabo, Vitruvius, Pliny, Palladius, and Antipater (*3*), may have supported this view. Over the past decades, however, numerous Roman mill sites have been discovered by archaeologists, and it has become clear that there was considerable innovation in Roman times, especially in the field of hydraulics and the use of watermills from the first century CE onward (*1*, *5*–*9*). A prominent, yet not widely known example of a technological masterpiece is preserved at Barbegal in southern France (Fig. 1, A and B), where a large water-powered grain mill complex was built in the second century CE (*10*–*12*). The Barbegal watermill complex is the earliest and largest known industrial utilization of hydropower by an ancient society. The complex, composed of 16 watermills (Fig. 1, C and D), has been described as "the greatest known concentration of mechanical power in the ancient world" (*1*, *5*) and has no equivalent either in the Roman world or in Asian civilizations, although both are known for their achievements in other fields of hydraulic engineering (*6*, *10*, *13*). Originally, it was believed that the mills of Barbegal were built at the end of the third century CE, when Arles was the residence of the Emperor Constantine, for the production of flour for the imperial administration, the army, and the city (*10*). The mills were previously used to illustrate a profound social change: With Christianization, the end of slavery liberated the inventive capacities of engineers and favored the use of natural energy, in this case, hydropower, to produce flour. However, excavations in the early 1990s led to the abandonment of this hypothesis (*11*) and recognized Barbegal as a unique, early climax of technological development.

[1]Department of Earth Sciences, Johannes Gutenberg University, 55128 Mainz, Germany. [2]Aix-Marseille Université, CNRS, Centre Camille Jullian, UMR 7299, 13094, Aix-en-Provence, France. [3]Institute of Geology, University of Innsbruck, Innrain 52, 6020 Innsbruck, Austria. [4]Université Rennes 1, CNRS, UMR 6566, CReAAH, Rennes, France.
*Corresponding author. Email: cpasschi@uni-mainz.de

Today, nearly 80 years after the first excavation of the complex (1937–1939), key questions still remain open: What was the destination of the large amount of flour produced by the mill complex? How did it function and for how long was it in use? And did mill complexes of this scale spread over the Roman Empire? These questions have remained unsolved because the ruins are only fragmentary, excavation records are incomplete (*10*), and only few other industrial sites of comparable scale are known in the Roman Empire. Here, we show that novel laboratory techniques and interdisciplinary research can shed new light on these long-standing questions.

Many Roman water supply systems were fed by karst springs with a high content of calcium and bicarbonate. These ions are kept in solution by enhanced P_{CO_2} (partial pressure of CO_2) and associated low pH values due to the passage of rainwater through the soil before entering the karst system. When the water leaves the karst spring, CO_2 degasses and, as a consequence, calcium carbonate precipitates both naturally in the form of tufa and on artificial structures of water management systems. Because the rate of deposition is influenced by the temperature, the chemical composition, and the flow rate of the water, the deposits form layers of different crystal structure and chemical and isotopic composition, creating a natural archive of past environmental conditions. Carbonate deposits from water supply systems fed by karst springs therefore not only are an established paleoenvironmental archive but also hold high promise as an archaeological resource. These deposits store information on water temperature, discharge, and composition, as well as on structural changes to the water systems, both natural (for example, damage by an earthquake or flooding) and artificial (for example, repair work of channels) (*14*–*16*).

In the collection of the Archaeological Museum of Arles, we found 142 fragments of carbonate deposits that stem from the first Barbegal excavations performed in the 1930s. These deposits had formed on (now decayed) wooden parts of the mills that had been in direct contact with flowing water. We examined these carbonate fragments macroscopically and microscopically and by means of stable isotope analysis. The microstratigraphy of the individual specimens provides unique new insights into the use of the mills, their maintenance, and the ultimate destruction of this industrial complex.

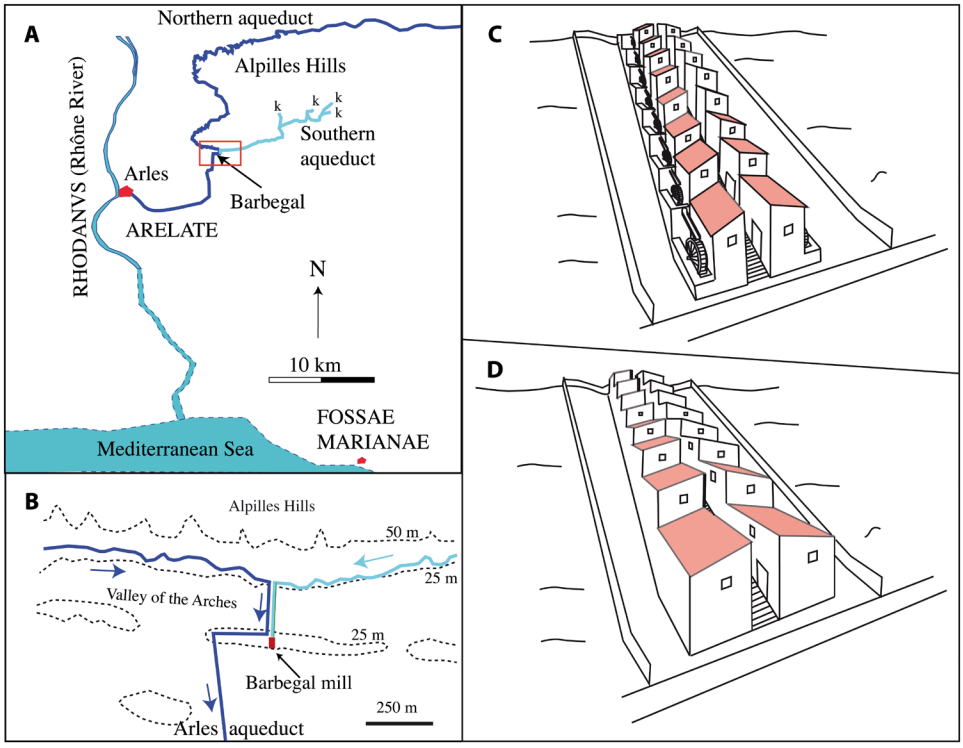

Fig. 1. Location and reconstruction of the Barbegal watermill complex. (**A**) Overview map. k, karst springs. (**B**) Detailed map of the small red rectangle in (A). The southern aqueduct (light blue) fed into the mill complex. Blue arrows indicate flow directions. Dotted lines: contour lines (m). (**C**) Proposed reconstruction of the complex, consisting of two parallel rows of watermills in open-air conditions, built on a hillslope. (**D**) Alternative reconstruction proposed in this study, where the watermills were enclosed within buildings.

RESULTS

Site description

The Barbegal mill complex (43°43.28′N, 004°43.17′E) was situated approximately 8 km northeast of the Roman city of Arelate, the modern city of Arles (Fig. 1, A and B). The complex consisted of two parallel rows of eight aligned watermills, fed by an aqueduct and with housings covering the grain mills (Fig. 1, C and D). The mills had an estimated production capacity of 25 metric tons of flour per day, enough to feed a population of at least 27,000 people (*5*). The 9-km-long mill aqueduct collected water from several small karst springs, located along the southern side of the Alpilles hills (southern aqueduct shown in Fig. 1A). Between 50 and 120 CE, this aqueduct was one of two channels providing water to the neighboring city of Arelate. Around 120 to 130 CE, the southern aqueduct was diverted to feed the newly constructed mill complex, while a new aqueduct branch was added on the north side of the hills to supply water to the city (Fig. 1A, northern aqueduct) (*10*, *11*). Thin tufa deposits occur close to the springs.

Macroscopic description of the carbonate deposits

A collection of carbonate fragments originating from the Barbegal mills was investigated in detail. The carbonate crusts are up to 65 mm thick and must have formed over several decades, showing that these deposits were not normally cleaned from the woodwork during operation and maintenance of the mill complex. The analyzed fragments still bear wood imprints (the "substrate") on one side, while the other side was in contact with water (Fig. 2). The fragments can be divided into two types: Large carbonate slabs that formed in millrun flumes that fed the water to the mill (Fig. 2, A to D) and deposits that had formed on the wooden parts of the actual water wheels (examples shown in Fig. 2, E and F). Calcite crystals grew perpendicularly to the surface of the substrate. The deposits growing in the millrun flumes formed a U-shaped profile. When the wood had decayed or had been removed, the deposits broke preferentially into planar fragments along 45° angles, allowing the identification and reassembly of individual flume fragments (Fig. 2, C and D). The flumes were 30 to 33 cm wide with sides of 17 to 22 cm high. The wood imprints bear evidence of resinous logs sawn tangentially into planks. Regular tool marks perpendicular to the longitudinal timber axis prove that these boards—as probably all lumbers used locally—were produced with mechanic saws using vertical blades, driven by watermills other than the Barbegal ones.

The deposits that had formed on the sides of flumes commonly terminated in an overhang, caused by water spilling over the sides at their tops (Fig. 2, B and D). These deposits are further characterized by a smooth, straight internal layering, which can be attributed to the continuous exposure to deeper water, as opposed to the more chaotic and incomplete deposits formed at sites characterized by discontinuous overflow. Other pieces have complex shapes or formed on thin planks, and they were probably part of the actual water wheels. Several fragments attributed to parts of the water wheel (for example, Fig. 2, E and F) show a rippled surface strongly resembling surface crenulations known from stalactites and stalagmites in caves, which result from small-scale instabilities within a water film (*17*). One fragment had a 45° conical top (Fig. 2G) and may have mantled a pole supporting a flume or part of the water wheel.

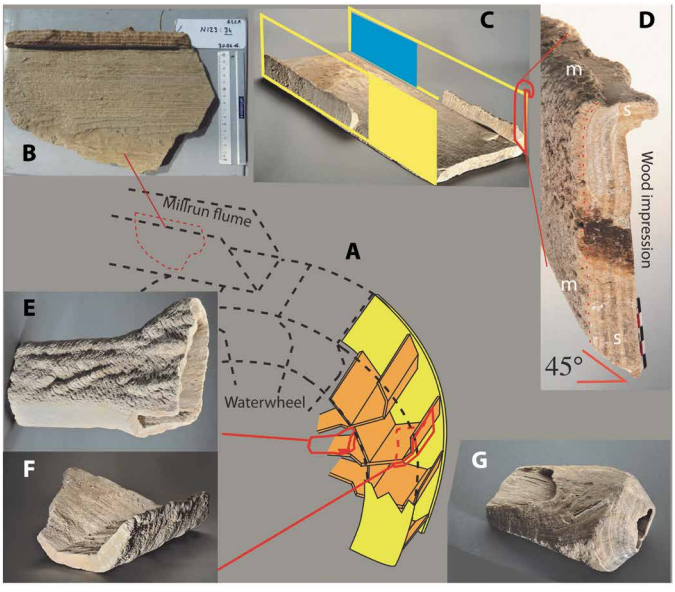

Fig. 2. Selected carbonate fragments from the woodwork of the Barbegal watermills and reconstruction of their original positions. (**A**) Possible reconstruction of a water wheel and flume based on the fragments found and other Roman watermill reconstructions (*26*, *40*). (**B**) Fragment N123, a slab from a flume sidewall with clear impressions of wood. (**C**) Fragment N140, representing the base of a millrun flume. The reconstruction of the flume shows the wood side in yellow and the water side in blue. The position of fragment N126 in a similar flume is indicated. (**D**) Fragment N126 from a side wall slab showing a 45° angle connecting the bottom and sides. The top (left side) of the deposits is micritic and porous (m), while the main deposit is sparitic (s); the sharp transition is marked by a red dashed line. (**E**) Fragment N81, which grew around a spoke of a water wheel, with a square-shaped opening where the slab had been attached. (**F**) Fragment N138, interpreted as the impression of the bucket of a water wheel. (**G**) Fragment N83, deposited around a wooden pole, as apparent from the central hole, with a conically shaped top, for which the original position remains unclear. Photographs by P.L.

The top cone suggests that it formed in contact with a large planar side of wood.

By using the geometry of the wood impressions, 93 of the 142 fragments could be attributed to millrun flumes and 43 to fragments of water wheels, while 6 are of uncertain origin or are too small to analyze. Twenty-five pieces were sectioned from small, archaeologically less important fragments for microstratigraphic analysis, while others were only cleaned and their stratigraphy was photographed on broken surfaces to preserve these unique specimens.

Microstratigraphy of the carbonate deposits

All carbonate fragments display a characteristic alternation of differently colored layers. Detailed comparisons performed on polished sections revealed that many fragments contained overlapping, matching microstratigraphies. The carbonate deposits fall into several microstratigraphic groups. Fragments from sides and floors of millrun flumes that formed simultaneously could be reassembled using this approach. Although the thickness of individual layers varies between fragments, probably due to minor in situ variation in water flow rate and turbulence, their succession and characteristics (color and crystal size) could be used successfully to align most of these pieces, even if they were deposited on different parts of the mill complex. In many cases, the microstratigraphy of millrun flume fragments matched that of pieces from water wheel parts, demonstrating contemporaneous deposition (Fig. 3). Fragments whose microstratigraphy only partly overlaps are particularly interesting, including fragments N109, N133, and N90 (Fig. 3, A to C). The microstratigraphy of these fragments shows three distinct sections (I, II, and III; Fig. 3D), which is complete in fragment N109, while fragment N90 preserves sections II and III, and fragment N133 only contains section III. The variable presence of these sections can be explained as follows.

Section I of fragment N109 started to grow first in a millrun flume during operation of the mills (Fig. 3B). Fragment N90 formed on a 5-cm-wide piece of wood attached to a wider wooden segment, probably from the mill wheel (Fig. 3, A and E). This segment was installed after the millrun flume, in which fragment N109 formed, had operated for several years. The deposits of fragment N90 (section II) were partly chipped off after some years of operation, resulting in an unconformity (Fig. 3A). This occurred at the same time as growth of fragment N133 commenced, which is part of a 30-cm-wide flume bottom deposit (Fig. 3, C and G). The unconformity is attributed to a repair process when the wood of fragment N133 was installed, while some activity took place on or near the site of fragment N90 (Fig. 3F). Deposition of section III in fragments N90, N109, and N133 then continued until carbonate deposition stopped, probably due to the termination of the mill operation (see below). This illustrates that repairs were carried out periodically and contemporaneously on different parts of the complex. The observation that these fragments only share part of the overall microstratigraphy can therefore be explained by repair activities.

Crystal structure

Microscopic analysis of the carbonate specimens revealed an alternation of sparite and microsparite (exemplified for fragment N133; Fig. 4, A and A2). The layering is more complex than that typically seen in carbonate deposits formed in aqueducts with continuously running water (*14*–*16*), where regular alternations of sparite and micrite form translucent and opaque layers, respectively. The sparite crystals in the Barbegal specimens from the flumes and basins form branching fans via growth competition, as in aqueducts, but the crystals are truncated, indicative of interruptions of the water flow (Fig. 4, A and A2) (*18*). Brown bands typical of high colloid load associated with heavy rainfall events (*18*) occur within and near the base of sparite fans (Fig. 4A2). Micrite bands are rare but occasionally cap sparite crystals, indicating temporarily low water levels and strongly reduced flow rates (*14*, *15*, *18*).

In open-air conditions such as rivers and channels, carbonate deposits usually form tufa, that is, micritic, porous deposits commonly containing casts of plant remains, except where the flow is fast enough to deter settlement of microorganisms and plants on the substrate (*15*, *19*–*23*). Carbonate deposits formed in modern watermills and in ancient mills in Venafro (*5*), Saepinum (*24*), Athens (*5*, *25*), and Ephesos (*26*) that functioned in open air (Fig. 1C) also show porous micritic deposits despite fast and highly turbulent water flow. In contrast, carbonate deposits formed on the Barbegal woodwork are unusually dense and sparitic for watermill deposits. The top 1 to 10 mm of the deposits, however, are composed of white, porous, micritic tufa-like carbonate with imprints of plants, that is, very different from the sparitic deposits beneath [for example, N126 (Fig. 2D), N133 (Figs. 3, C and G, and 4, A and A1), and N90 and N109 (Fig. 3, A, B, and E)].

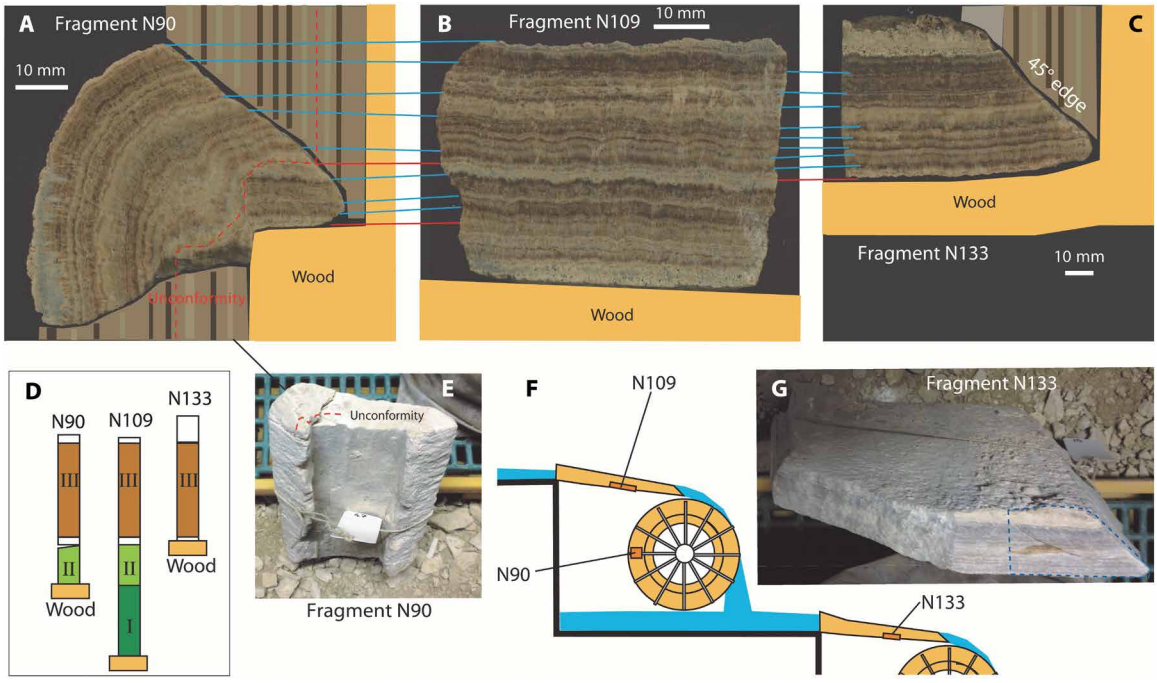

Fig. 3. Microstratigraphic correlation of carbonate fragments. (**A** to **C**) Fragments N90, N109, and N133 with a reconstruction of originally attached wood and adjacent deposits. Blue and red lines connect layers in the three fragments that were formed simultaneously, although the fragments were not part of a continuous deposit and the thickness of the layered calcite deposits differs among the three fragments. Fragments N109 and N133 are shown at different scales. The red dashed line marks an unconformity. (**D**) Schematic presentation of the microstratigraphy of the three fragments, with variably present microstratigraphic sections I, II, and III. Section III is present in all three fragments, section II is only present in fragments N90 and N109, and section I is exclusively present in fragment N109. This is attributed to different growth periods for each fragment, N109 being the most complete and N133 being the least complete. All three fragments were capped by porous calcite of variable thickness, indicated in white. (**E**) Fragment N90 formed on part of a wheel, and the negative wood imprint is clearly visible. The top left corner was polished and is shown in (A). (**F**) Schematic reconstruction of the millwheels and flumes showing possible locations of the three fragments. (**G**) Fragment N133 originates from the bottom of a millrun channel. The fragment shown in (C) was taken from the front as indicated by a blue dashed line. Photographs by C.W.P.

Stable isotope composition

Stable isotope analyses of oxygen and carbon were performed on selected carbonate fragments. This method has previously been applied to carbonate deposits from ancient and modern aqueducts, demonstrating that sinusoidal, mirror-like oscillations of $\delta^{18}O$ and $\delta^{13}C$ reflect seasonal variations in the conditions of carbonate precipitation (Fig. 4, C and D) (*14*–*16*). Variation in $\delta^{18}O$ is attributed to isotope fractionation in response to seasonal changes in water temperature in the channel, whereby high $\delta^{18}O$ values represent cold water during winter and low values represent warm summer water (Fig. 4D) (*14*–*16*, *18*). $\delta^{13}C$ values primarily reflect variable degassing in response to seasonal water-level changes (*14*–*16*). High levels in the channel due to high rainfall in winter and spring are thought to correlate with restricted degassing and low $\delta^{13}C$ values in these seasons (*14*–*16*, *18*). $\delta^{18}O$ values gradually decrease across spring and summer, while $\delta^{13}C$ values increase (Fig. 4C). This trend reflects calcite precipitation at progressively higher temperatures and decreasing discharge, promoting degassing. In the Barbegal carbonate fragments, both isotope values are hence mostly anticorrelated, with a clearly visible seasonal signal that correlates with the petrographic layering. The shape of both $\delta^{18}O$ and $\delta^{13}C$ curves, however, is irregular and skewed, with steep truncated slopes on increasing legs of the curve (Fig. 4, A and B). At least 6 of a total of 16 cycles of such a truncated pattern are recorded in fragment N133 (Fig. 4A). The truncated pattern is independently confirmed by the longer microstratigraphy of fragment N109, where 11 truncated cycles are preserved and 6 truncated cycles occur bound to the same levels in the shared part of the stratigraphy (Fig. 4B). Such a truncated pattern in $\delta^{18}O$ and $\delta^{13}C$ from carbonate deposits of aqueducts has not been reported elsewhere and is attributed to interruptions in the use of the water system (Fig. 4, E and F). Considering the asymmetrical geometry of truncated cycles in Fig. 4 (A and B), we conclude that the operation of the mill was regularly interrupted for several months. On the basis of the position within the annual cycle, interruptions occurred predominantly in late summer and autumn. Operation commenced again in winter, as indicated by the sharp increase in $\delta^{18}O$ representative of cooler water temperatures and/or wet periods (Fig. 4, A and B). At these points in the stratigraphy, thin bands of micrite cap older sparite and competitive growth of sparite crystals is present, typical of renewed growth of calcite after a dry period: This reflects the reactivation of the mills (Fig. 4A2) (*18*).

DISCUSSION

A comparison of the microstratigraphy of coeval fragments (Fig. 3) reveals clear evidence of maintenance of the Barbegal mills and shows that wooden structures were replaced approximately every 5 to 10 years, dictated by the rate of mold and decay. Periodic maintenance is known from medieval mills and was typically required at these intervals (*27*).

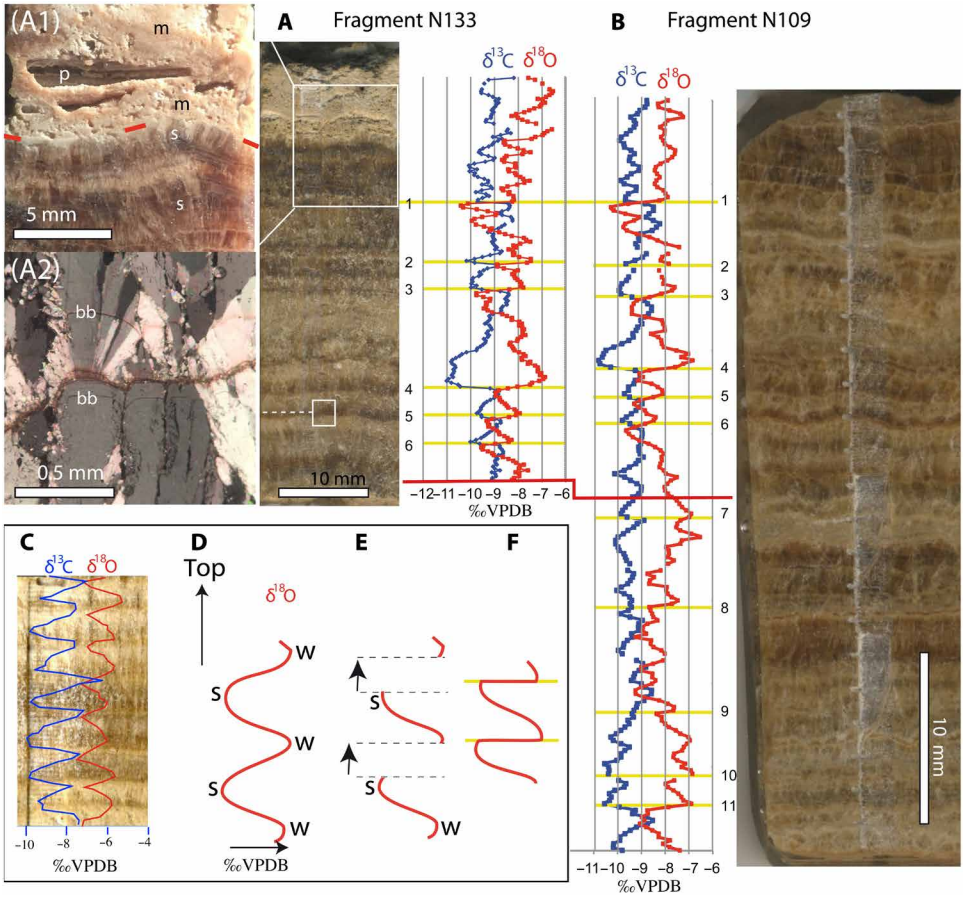

Fig. 4. Stable isotope composition of representative carbonate fragments N133 and N109 from the Barbegal mills. (**A**) Sample of fragment N133 with micromill trace and associated stable isotope profile. Position of close-ups (A1) and (A2) marked by white squares. The sample is mostly sparitic with a sharp transition to a micritic top. Fragment N133 yielded irregular truncated isotope curves. Yellow lines mark the truncation sites where operation of the mills was likely interrupted. (A1) Close-up of the side of (A) showing a sharp transition, marked with red lines, from dense sparite (s) to porous micrite (m) with plant imprints (p), formed from decayed plant matter at the top of N133. (A2) Thin-section image of truncation surface #5 in sparite of sample N133, coinciding with a truncation in the stable isotope curves. bb, brown bands in sparite. Crossed polarized light. (**B**) The isotope pattern of N133 was replicated in fragment N109 and has a longer stratigraphy than fragment N133. Red line in (A) and (B) marks the same stratigraphic level in the stable isotope graphs. (**C**) Comparison of a carbonate deposit from the Roman aqueduct of Aspendos (Turkey) showing a highly symmetrical pattern [modified after (*14*)], whose $\delta^{18}O$ cyclicity is attributed to seasonal, temperature-controlled isotope fractionation (**D**). W, winter; S, summer. (**E**) The Barbegal stable isotope time series record interruptions, mostly during late summer and autumn, giving rise to truncated curves (**F**), marked by yellow lines in (A) and (B). VPDB, Vienna PeeDee Belemnite. Photographs by C.W.P.

The sparitic and dense nature of the bulk of the carbonate deposits of Barbegal is strikingly different from the porous deposits of modern or ancient watermills (*23*–*26*). This sparite is overgrown by porous micrite with imprints of plant remains, reflecting a fundamental and sudden change in depositional conditions (Fig. 4A1). The porous top layer, occupying the entire depth of the fully operating and overflowing flumes (Fig. 2D), was deposited at a rate similar to that of the underlying dense deposits (Fig. 4A) and was therefore formed at similar water depth and flow speed. This suggests that the flow regime did not change during and after the fabric transition.

The stable isotope cyclicity continues across the petrographic boundary, suggesting that the depositional conditions of the micrite lasted for at least 1 year. Both $\delta^{18}O$ and $\delta^{13}C$ values increase slightly, while the regular cyclicity is maintained (Fig. 4A). For $\delta^{18}O$, this could indicate an increase in evaporation, while for $\delta^{13}C$ the increase could be due to increased degassing or photosynthetic activity of plants in the water. We believe that light was the key factor causing the change in fabric, with initial deposition in dark conditions, hampering growth of photosynthetic organisms, followed by a sudden change near the end of the depositional history toward biogenically dominated calcite precipitation. The fabric of the main deposits is identical to calcite formed in closed aqueduct channels with fast flowing water (*13*–*16*, *18*). This suggest that the Barbegal mills either were shaded by overhanging roofs or, more likely, were enclosed within buildings during the formation of dense sparite (Fig. 1D), and that these structures were partly removed or collapsed during the final phase of porous carbonate deposition. As a result, the water mills were exposed to sunlight, triggering the growth of photosynthetically active organisms. Deposits in the feeding aqueduct of the mills are exclusively sparitic and do not show a petrographic change.

Operation of the waterwheels inside buildings may also explain why the carbonate deposits were not regularly removed from the

woodwork: For a 2-m-long wooden flume consisting of 2-cm-thick pine wood boards with a weight of 15 to 20 kg, a 5-cm-thick carbonate crust as in Fig. 3 would have added 170 kg to its total mass. Regular removal of this material may have been impaired by the closed nature of the wheel chambers (Fig. 1D).

Stable isotope analyses of carbonate deposits shed light on the mode of operation and purpose of the Barbegal mill complex. Despite the truncated nature of the isotope pattern, the seasonal cyclicity is well preserved. The number of cycles indicates that, for instance, fragment N133 covers 16 to 17 years of mill operation, while fragment N109 was formed during a period of up to 30 years (Fig. 4B). The asymmetrical shape of the isotope curves strongly suggests that the mills were not used continuously throughout the year. Instead, operation was halted, mostly in late summer and autumn. It can be ruled out that this truncated isotope pattern was caused by regular repair activities, as they would not have depended on a regular yearly pause in operation.

In most of the ancient world, milling of grain was done locally at home, in bakeries, or in individual watermills, which seem to have been common from the first century CE onward (*6*, *8*). Flour was produced close to the end user, mostly because it had a shorter shelf life than unmilled grain. Barbegal stands out because of its unusual size and capacity (*11*, *12*).

Because of the vicinity of the Roman city of Arelate, it was originally proposed that the mills of Barbegal provided flour for the entire population of this city (*5*, *12*). However, the annual interruption of mill activity revealed by the stable isotope data is difficult to reconcile with a continuous year-round demand for flour to a city. Transport of large quantities of flour over long distances or months-long storage seems unlikely because of spoilage. An alternative explanation, that the mills were used to produce flour for the army, is unlikely because no large military concentration is known from the area for the period of activity of the mills.

The proximity of the major ports of Arles and Fossae Marianae (Fig. 1A) suggests an alternative destination of the massive amounts of flour produced by the Barbegal complex: It may have been used for the production of ship's bread (*panicus panis*) meeting the needs of ships that frequented these ports. *Panis nauticus*, equivalent to *panis militaris* or *buccelatum* (*28*–*30*), was a major staple aboard ships. After it was double baked, it was suitable for long-term storage, just like ship's bread typically used in later periods. A similar situation has been proposed to explain the large number of bakeries in Ostia, the harbor city of ancient Rome (*31*). In modern times, in the mouth of the river Tagus (Portugal), a concentration of more recent tidal mills supplied flour to the hardtack factories for the navy and the Company of India as well as for local fortifications (*32*). Hardtack could be produced in large quantities, stored, and transported over long distances. Moreover, as Roman shipping activities typically halted in late autumn, its production would have peaked in spring and early summer, to be halted in late summer when the demand ceased. This is in accordance with the cyclical period of operation of the Barbegal mills.

The use of the Barbegal complex seems to have ended after a sudden exposure of the structures to sunlight, leading to the formation of tufa-like calcite capping the dense crystalline deposit in the still working flumes, before the mills were finally abandoned (Fig. 4, A and A1). In these last porous deposits, imprints of fragments of worked wood and other debris are common, suggesting that the active operational period of the mills ended in a non-structured manner by lack of proper maintenance. This event is dated to the early third century CE (*11*). At that time, an economic crisis associated with military and political turmoil affected the Roman Empire (*33*), which likely led to the abandonment of this industrial mill complex.

Up to the late 20th century, the Roman economy was envisaged as slave-based (*2*, *3*), and the use of watermills was grossly underestimated. This partly stems from a lack of archaeological observations: Excavations have long been focused on allegedly important sites of religious and political nature in urban centers rather than on technologically complex and economically more important but less impressive buildings such as watermills. Mills are also vulnerable structures, commonly located outside archaeological key sites, and can easily be overlooked or misinterpreted (*6*, *8*). Over the past decades, however, the archaeological focus has shifted, and an increasing number of watermill remains have been excavated (*6*–*8*, *34*). It is now well established not only that Greco-Roman society excelled in hydraulic engineering (*5*, *6*, *13*) but also that a veritable revolution of waterpower affected the Roman Empire between the first and the third century CE (*8*, *9*, *35*–*37*).

Unfortunately, the archaeological record provides only tantalizing glimpses of the progress in mill development during Roman times. Numerous small grain mills associated with villas were found over the past decades (*34*). Several examples of Roman tidal mills were recognized in England (*5*). A late third or early fourth century CE complex of advanced helix-turbine watermills was found at Chemtou and Testour (Tunisia), a technology only seen again in the 16th century in Spain (*36*). Late Roman stone-cutting watermills were found in Jordan and Turkey (*38*), while an antique description exists from Germany by Ausonius (*38*). Sawmills for wood using vertical blades also existed, as first shown by the wood imprints described in this study. There is also evidence for the use of mills in the processing of ore and other applications (*6*). Among these examples, however, Barbegal stands out as the oldest preserved industrial-scale complex in history.

One century after the construction of Barbegal, in the third century CE, a group of watermills was built on the Janiculum Hill in Rome, fed by the Traiana and Alsietina aqueducts (*9*, *35*). These mills were constructed when the distribution of grain to parts of the population of Rome was replaced with bread (*8*, *9*, *35*, *37*). The mills were probably built to supply flour for public bakeries, previously produced by muscle power (*35*). Similar complexes may have existed in other cities from the third century onward (*8*, *39*). Unfortunately, knowledge of the distribution of watermill complexes and their role in the Roman economy is still highly fragmentary. Among watermills, Barbegal marks the climax in the second century CE of Roman mill technology, but to what extent it contributed to the further spread of mill technology and mill complexes during and after the second century CE is presently unknown.

With the insights gained by the study on Barbegal, future research should be focused on other large watermill complexes and will likely change our perception of industrial growth during Roman times. Watermill complexes like Barbegal and the Janiculum depended on a large market for flour and a suitable water supply. Because both the location of large urban centers and harbors in the Roman Empire, as well as the sites of large aqueducts and their springs, are known, it should be possible to predict the locations of further large and hitherto undiscovered mill complexes.

METHODS

Sample preparation

Twenty-four carbonate samples were cleaned and cut with a Makita BGA452Z angle grinder and a 1-mm-wide and 115-mm-diameter diamond saw blade. Samples were polished on one side using diamond abrasive paste in the thin-section laboratory in Mainz using standard procedures.

Microscopy

The calcite microstructure was investigated in 21 polished thin sections and examined using a Leica petrographic microscope in the optical laboratory in Mainz.

Stable isotope analysis

Samples were cut using a thin bronze diamond saw, and mirror image halves were used to produce either polished thin sections or polished slabs. This approach guaranteed comparability of microstructures in thin section with macroscopically visible layering and stable isotope milling traces. Following microstructure investigation using transmitted light microscopy, the least porous and regularly laminated parts of samples were selected for micromilling. Each polished slab was micromilled at 0.2-mm intervals along four parallel and 5-mm-wide traverses perpendicular to the lamination using a Merchantek micromill (ESI New Wave). Sample powders were analyzed using a semiautomated device (GasBench II, Thermo Fisher) linked to a Thermo Fisher Delta^{plus}XL isotope ratio mass spectrometer. Isotope values were reported on the VPDB scale, and long-term precision was <0.1‰ for both $\delta^{13}C$ and $\delta^{18}O$. All stable isotope analyses were carried out at the University of Innsbruck. Standardization of the mass spectrometer was achieved using international calcite standards, including NBS18, NBS19, CO1, and CO8.

SUPPLEMENTARY MATERIALS

Supplementary material for this article is available at http://advances.sciencemag.org/cgi/content/full/4/9/eaar3620/DC1

Fig. S1. Sample of fragment B3 from the wall of mill basin E4, with micromill trace and associated stable isotope profile.

Stable isotope data as presented in Fig. 4 and fig. S1.

REFERENCES AND NOTES

1. K. Greene, Technological innovation and economic progress in the ancient world: M.I. Finley re-considered. *Econ. Hist. Rev.* **53**, 29–59 (2000).
2. M. I. Finley, Technical innovation and economic progress in the ancient world. *Econ. Hist. Rev.* **18**, 29–45 (1965).
3. T. S. Reynolds, *Stronger Than a Hundred Men: A History of the Vertical Waterwheel* (Johns Hopkins Studies, 1983).
4. A. Schiavone, *The End of the Past: Ancient Rome and the Modern West (Revealing Antiquity)*, M. J. Schneider, Transl. (Harvard Univ. Press, 2000).
5. J. R. Spain, *The Power and Performance of Roman Water-Mills: Hydro-Mechanical Analysis of Vertical-Wheeled Water-Mills*, British Archaeological Reports (BAR) International Series, vol. S1786 (John and Erica Hedges Limited, 2008).
6. Ö. Wikander, *Handbook of Ancient Water Technology* (Brill Academic Publishers, 2000).
7. A. R. Lucas, *Wind, Water, Work: Ancient and Medieval Milling Technology* (Brill Academic Publishers, 2011).
8. Ö. Wikander, Sources of energy and exploitation of power, in *The Oxford Handbook of Engineering and Technology in the Classical World*, J. P. Oleson, Ed. (Oxford Univ. Press, 2008), pp. 136–152.
9. A. Wilson, Machines, power and the ancient economy. *J. Roman Stud.* **92**, 1–32 (2002).
10. F. Benoit, L'usine de meunerie hydraulique de Barbegal (Arles). *Revue Archéol.* **15**, 19–80 (1940).
11. P. Leveau, Les eaux des Alpilles, la colonie romaine d'Arles et les moulins de Barbegal. Un système hydraulique et ses paradigmes interprétatifs, Les réseaux d'eau courante dans l'Antiquité, in *Les Réseaux d'Eau Courante Dans l'Antiquité*, C. Abadie-Reynal, S. Provost, P. Vipard, Eds. (Presses Universitaires de Rennes, 2011), pp. 115–132.
12. R. H. J. Sellin, The large Roman water mill at Barbegal (France). *Hist. Technol.* **8**, 91–109 (1983).
13. A. T. Hodge, *Roman Aqueducts and Water Supply* (Duckworth, 1992).
14. G. Sürmelihindi, C. W. Passchier, C. Spötl, P. Kessener, M. Bestmann, D. E. Jacob, O. H. N. Baykan, Laminated carbonate deposits in Roman aqueducts: Origin, processes and implications. *Sedimentology* **60**, 961–982 (2013).
15. G. Sürmelihindi, C. W. Passchier, O. N. Baykan, C. Spötl, P. Kessener, Environmental and depositional controls on laminated freshwater carbonates: An example from the Roman aqueduct of Patara, Turkey. *Palaeogeogr. Palaeoclim. Palaeoecol.* **386**, 321–335 (2013).
16. C. Passchier, G. Sürmelihindi, C. Spötl, A high-resolution palaeoenvironmental record from carbonate deposits in the Roman aqueduct of Patara, SW Turkey, from the time of Nero. *Sci. Rep.* **6**, 28704 (2016).
17. C. Camporeale, L. Ridolfi, Hydrodynamic-driven stability analysis of morphological patterns on stalactites and implications for cave paleoflow reconstructions. *Phys. Rev. Lett.* **108**, 238501 (2012).
18. C. Passchier, G. Sürmelihindi, C. Spötl, R. Mertz-Kraus, D. Scholz, Carbonate deposits from the ancient aqueduct of Béziers, France—A high-resolution palaeoenvironmental archive for the Roman Empire. *Palaeogeogr. Palaeoclimat. Palaeoecol.* **461**, 328–340 (2016).
19. A. Pentecost, *Travertine* (Springer, 2005)
20. T. D. Ford, H. M. Pedley, A review of tufa and travertine deposits of the world. *Earth Sci. Rev.* **41**, 117–175 (1996).
21. H. M. Pedley, Classification and environmental models of cool freshwater tufas. *Sediment. Geol.* **68**, 143–154 (1990).
22. M. Gradzinski, Factors controlling growth of modern tufa: Results of a field experiment, in *Tufas and Speleothems: Unravelling the Microbial and Physical Controls*, H. M. Pedley, M. Rogerson, Eds. (Geological Society, 2010), vol. 336, pp. 143–191
23. M. Pedley, Freshwater (phytoherm) reefs: The role of biofilms and their bearing on marine reef cementation. *Sediment. Geol.* **79**, 255–274 (1992).
24. J. L. Guendon, Les concrétions du canal d'amenée d'eau au moulin: examen pétrographique, in *Les installations artisanales Romaines de Saepinum. Tannerie et moulin hydraulique*, J.-P. Brun, M. Leguilloux, Eds. (Collection du Centre Jean Bérard, CNRS, 2014), vol. 43, pp. 131–135.
25. A. W. Parsons, A Roman water-mill in the Athenian Agora. *Hesperia* **5**, 70–90 (1936).
26. C. Passchier, G. Sürmelihindi, Geochemical observations on sinter of Ephesos, in *Die Mühlenkaskade von Ephesos*, S. Wefers, Ed. (Verlag des Römisch-Germanischen Zentralmuseums, 2015), pp. 120–123.
27. J. Rouillard, L'apport des sources écrites à l'archéologie du Moulin à eau medieval, in *Archéologie des Moulins hydrauliques, à traction animale et à vent, des origines à l'époque médiévale*, L. Jaccottey, G. Rollier, Eds. (Annales Littéraires de l'Université de Franche-Comté, 2016), vol. 959, 2, pp. 531–548.
28. J. P. Roth, *The Logistics of the Roman Army at War (264 B.C.-A.D. 235)* (Brill Academic Publishers, 1999), pp. 51–53.
29. N. George, Bucellatum—Roman Army Hardtack (2014); http://pass-the-garum.blogspot.de/2014/10/bucellatum-roman-army-hardtack.html.
30. M. Junkelmann, *Panis Militaris: Die Ernährung des römischen Soldaten oder der Grundstoff der Macht* (Von Zabern, 1997).
31. C. DeRuyt, Boulangers et foulons d'Ostie à l'époque impériale. Quelques réflexions sur l'implantation de leurs ateliers et sur leurs fonctions précises dans la ville portuaire, in *Les Artisans Dans La Ville Antique*, J. C. Béal, J. C. Guyon, Eds. (Diffusion de Bockard, 2002), pp. 49–53.
32. H. Wittenberg, Gezeitenmühlen im Portugal, in *Hamburg, die Elbe und das Wasser sowie weitere wasserhistorische Beiträge*, C. Ohlig, Ed. (Schriften der Deutschen Wasserhistorischen Gesellschaft, 2009), vol. 13, pp. 185–196.
33. A. Watson, *Aurelian and the Third Century* (Taylor & Francis, 2003).
34. A. Wilson, Water, power and culture in the Roman and Byzantine worlds: An introduction. *Water Hist.* **4**, 1–9 (2012).
35. Ö. Wikander, "Where of old all the mills of the city have been constructed". The capacity of the Janiculum mills in Rome, in *Ancient History Matters*, K. Ascani, V. Gabrielsen, K. Kvist, A. H. Rasmussen, Eds. (Analecta Romana Instituti Danici, suppl. 30, 2002), pp. 127–133.
36. A. I. Wilson, Water-power in North Africa and the development of the horizontal water-wheel. *J. Roman Archaeol.* **8**, 499–510 (1995).
37. A. Wilson, The Water-Mills on the Janiculum. *Mem. Am. Acad. Rome* **45**, 219–246 (2000).
38. P. Kessener, Stone sawing machines of Roman and early Byzantine times in the Anatolian Mediterranean. *Adalya* **13**, 283–304 (2010).
39. A. Wilson, Late antique water-mills on the Palatine. *Pap. Br. Sch. Rome* **71**, 85–109 (2003).
40. C. Varoqueaux, J. M. Gassend, La roue à aubes du grand bassin de la Bourse à Marseille, in *Techniques et Sociétés en Méditerranée*, J. P. Brun, P. Jockey, Eds. (Maisonneuve & Larose, 2001).

Acknowledgments: We thank T. Wassenaar for editorial assistance. We wish to thank the Musée Départemental de l'Arles Antique, notably A. Charron and V. Clenas, for permission to study the samples and assistance during visits. We thank HYDRΩMED and S. Bouffier for general support and the Parc Naturel Regional des Alpilles for access to the Barbegal site. A. Wilson and R. Spain are thanked for discussion. We also appreciate the support of M. Wimmer in the isotope lab. **Funding:** This work was partially funded by the Deutsche Forschungsgemeinschaft, project 578/17, and by the University of Mainz (Stufe I). **Author contributions:** G.S. and C.W.P. set up and coordinated the project and cataloged and investigated the fragments in the Arles museum. G.S. carried out microstructural and stable isotope analyses and provided core interpretations. C.S. is the leader of the stable isotope laboratory in Innsbruck, where the core of this research was carried out. He supervised the stable isotope analyses and contributed to paper writing. P.L. and V.B. provided archaeological and dendrochronology expertise. C.W.P. made the drawings and set up the paper. The text was written with assistance from all authors. Photographs in Fig. 2 are by P.L. All other photographs are by C.W.P. **Competing interests:** The authors declare that they have no competing interests. **Data and materials availability:** All data needed to evaluate the conclusions in the paper are present in the paper and/or the Supplementary Materials. Additional data related to this paper may be requested from the authors.

Submitted 30 October 2017
Accepted 17 July 2018
Published 5 September 2018
10.1126/sciadv.aar3620

Citation: G. Sürmelihindi, P. Leveau, C. Spötl, V. Bernard, C. W. Passchier, The second century CE Roman watermills of Barbegal: Unraveling the enigma of one of the oldest industrial complexes. *Sci. Adv.* **4**, eaar3620 (2018).